

## Pseudo-half-metallicity in the double perovskite $\text{Sr}_2\text{CrReO}_6$ from density-functional calculations

G. Vaitheeswaran<sup>a)</sup> and V. Kanchana

*Max-Planck-Institut für Festkörperforschung, Heisenbergstrasse 1, 70569 Stuttgart, Germany*

A. Delin

*Materialvetenskap, Brinellvägen 23, KTH, SE-10044 Stockholm, Sweden*

(Received 13 September 2004; accepted 10 December 2004; published online 14 January 2005)

The electronic structure of the spintronic material  $\text{Sr}_2\text{CrReO}_6$  is studied by means of full-potential linear muffin-tin orbital method. Scalar relativistic calculations predict  $\text{Sr}_2\text{CrReO}_6$  to be half-metallic with a magnetic moment of  $1 \mu_B$ . When spin-orbit coupling is included, the half-metallic gap closes into a pseudo-gap, and an unquenched rhenium orbital moment appears, resulting in a significant increase of the total magnetic moment to  $1.28 \mu_B$ . This moment is significantly larger than the experimental moment of  $0.9 \mu_B$ . A possible explanation of this discrepancy is that the anti-site disorder in  $\text{Sr}_2\text{CrReO}_6$  is significantly larger than hitherto assumed. © 2005 American Institute of Physics. [DOI: 10.1063/1.1855418]

The family of magnetic oxides with an ordered double perovskite structure are complex materials with high technological potential in the area of spin electronics. Double perovskites have the general formula  $\text{A}_2\text{BB}'\text{O}_6$ , where A can be an alkali metal such as strontium, calcium, or barium, or a lanthanide, and B and B' are transition metals. Each transition metal site is surrounded by an oxygen octahedron (sometimes heavily distorted), and the A atoms are situated in the holes produced by eight adjacent oxygen octahedra.

In 1998, it was discovered that one such double perovskite,  $\text{Sr}_2\text{FeMoO}_6$ , possesses intrinsic tunneling-type magnetoresistance at room temperature—until then only observed in the mixed-valent manganese oxides<sup>1</sup>—making it a hot candidate material for spin-electronics applications.<sup>2</sup> The physical origin of the magnetoresistance in  $\text{Sr}_2\text{FeMoO}_6$  and in the mixed-valent manganese oxides is half-metallicity, i.e., the material is an insulator in one of the spin channels, but a metal in the other. This leads to a complete spin polarization at the Fermi level, which in turn results in strongly spin-dependent scattering of the charge carriers and thus a possibility to influence the resistance using relatively weak magnetic fields. Prerequisites for realizing high-performance devices using these materials are that the half-metallicity to a high degree is preserved at ambient temperature, and that high quality thin films of the material can be grown.

In this letter, we investigate the electronic structure of the double perovskite  $\text{Sr}_2\text{CrReO}_6$  using density functional theory. This system is particularly interesting since it exhibits the hitherto largest Curie temperature  $T_C$  of all known double perovskites, 635 K,<sup>3</sup> which is a couple of hundred kelvin higher or more than for  $\text{Sr}_2\text{FeMoO}_6$  (Ref. 4) as well as for the mixed-valent manganese oxides.  $\text{Sr}_2\text{CrReO}_6$  is a metallic ferromagnet with a saturation magnetic moment of around  $0.9 \mu_B$  per formula unit. At room temperature, the moment is only slightly reduced to around  $0.8 \mu_B$ , and high quality thin films of  $\text{Sr}_2\text{CrReO}_6$  can be produced in quite a large temperature window.<sup>3,5</sup> Thus, this material appears to satisfy important technological criteria. The measured saturation moment is quite well reproduced by a simple ionic picture of the

$\text{Sr}_2\text{CrReO}_6$  system, although this model takes neither hybridization nor orbital moments into account. In the ionic model, the Cr ions, situated on the B sites, have a  $3d^3$  configuration, leading to a moment of  $3 \mu_B$  antiferromagnetically coupled to the neighboring Re ions on the B' sites, with configuration  $5d^2$  or  $2 \mu_B$  per atom. In total, this gives a saturation spin moment of  $1 \mu_B$  per formula unit in the case of perfect ordering.

The present density-functional calculations were performed using an all-electron full potential linear muffin-tin orbital method (FP-LMTO), which has been described in detail elsewhere.<sup>6</sup> In this method, space is divided into non-overlapping muffin-tin spheres surrounding the atoms, and an interstitial region. Most important, this method assumes no shape approximation of the potential, wave functions, or charge density. Spin-orbit coupling was included in our calculations. The spherical-harmonic expansion of the potential was performed up to  $l_{\text{max}}=6$ , and we used a double basis so that each orbital is described using two different kinetic energies in the interstitial region. Furthermore, we included several pseudo-core orbitals in order to further increase accuracy. Thus, the basis set consisted of the Sr ( $4s 5s 4p 5p 4d$ ), Cr ( $4s 3p 4p 3d$ ), Re ( $6s 5p 6p 5d$ ), and O ( $2s 2p$ ) LMTOs. We performed our calculations using the experimentally determined structure and atomic positions, i.e., the tetragonal structure with space group symmetry  $I4/mmm$ , with cell parameters  $a=b=5.52 \text{ \AA}$ , and  $c=7.82 \text{ \AA}$ .<sup>3</sup> The radii of the muffin-tin spheres were  $2.68a_0$  for Sr,  $2.0a_0$  for Cr,  $1.98a_0$  for Re, and  $1.6a_0$  for O, respectively. The direction of the spin magnetic moment was chosen to be along the  $c$  axis. The integration in reciprocal space was performed using 376  $k$ -points in the irreducible Brillouin zone (BZ), corresponding to 2744 points in the full BZ for our self-consistent ground-state calculation. We tried both the local spin density approximation<sup>7</sup> and the generalized gradient approximation (GGA)<sup>8</sup> to the exchange-correlation functional. In the following, we will concentrate on our GGA results with the spin-orbit coupling included.

Our calculations reveal two important features of the electronic structure of  $\text{Sr}_2\text{CrReO}_6$ . First, our calculated total magnetic moment  $J_z$ , i.e., the sum of the spin and orbital

<sup>a)</sup>Electronic mail: g.s.vaithee@fkf.mpg.de

TABLE I. Calculated spin and orbital  $d$  magnetic moments in  $\mu_B$ /atom for  $\text{Sr}_2\text{CrReO}_6$ , with and without spin-orbit coupling (SO) included, and for different choices of the exchange-correlation functional. The total moment includes also the small spin and orbital moments present in non- $d$  orbitals, and the spin moment in the interstitial region.

	Spin		Orbital		Total
	Cr	Re	Cr	Re	
LSDA	2.00	-0.75			1.00
LSDA+SO	2.02	-0.69	-0.029	0.17	1.31
GGA	2.24	-0.90			1.00
GGA+SO	2.25	-0.85	-0.030	0.18	1.28
Ionic picture	3	-2			1

moments, at perfect ordering of the Cr and Re atoms, is about  $1.28 \mu_B$  per formula unit when spin-orbit coupling is included, i.e., a 28% larger magnetic moment than the one predicted by the ionic picture. (See Table I.) Second, we find that  $\text{Sr}_2\text{CrReO}_6$  is in fact not a perfect half metal. Let us discuss the magnetic moment first. When spin-orbit coupling is neglected, we find the total spin moment to be precisely  $1 \mu_B$ . With spin-orbit coupling included, the spin moment increases to  $1.1 \mu_B$ . Our calculated spin and orbital Cr and Re  $d$  moments are listed in Table I. Note that a large part of the spin moment is delocalized into the interstitial region, and therefore the individual  $d$  spin moments of the individual Cr and Re atoms inside their respective muffin-tin spheres in Table I appear small compared to the ionic values.

We find a Re  $5d$  orbital moment of around  $0.18 \mu_B$  and a total orbital moment of also  $0.18 \mu_B$ , calculated by summing up the orbital moments in all muffin-tin spheres. Both Cr and Re have less than half-filled  $d$  shells, and therefore the orbital moment is antiparallel to the spin moment for both species. Since the Cr and Re spin moments couple in antiparallel, the net result is that the total orbital moment, dominated by the Re orbital moment, is parallel to the total spin moment which, in turn, is dominated by the Cr spin moment. Consequently, the orbital moment has the effect of further increasing the total magnetic moment in this system.

Thus, when spin-orbit coupling is taken into account, our total predicted magnetic moment becomes significantly larger than what experimental studies indicate, and also larger than what the ionic model of  $\text{Sr}_2\text{CrReO}_6$  suggests.<sup>9</sup> Evidently, the spin-orbit effect is very important in this compound, which is hardly surprising since even in the case of elemental Re metal, the spin-orbit coupling is necessary in order to reproduce the experimentally observed band structure and Fermi surface.<sup>10</sup> What is surprising on the contrary is that the experimentally found moment is so close to the ionic value. A possible explanation for this paradox is that the anti-site disorder might be significantly larger in this system than previously assumed. One way to resolve this issue would be to determine the individual atomic spin and orbital moments in this system experimentally by performing, e.g., x-ray magnetic circular dichroism experiments.

We now turn to the question of half-metallicity in  $\text{Sr}_2\text{CrReO}_6$ , at perfect ordering. In our scalar-relativistic calculations, we indeed find a gap of 0.7 eV in the majority spin channel (see the top panel of Fig. 1), but when spin-orbit coupling is included, the band gap disappears and turns into a pseudo-gap with a low but finite density of states (DOS),

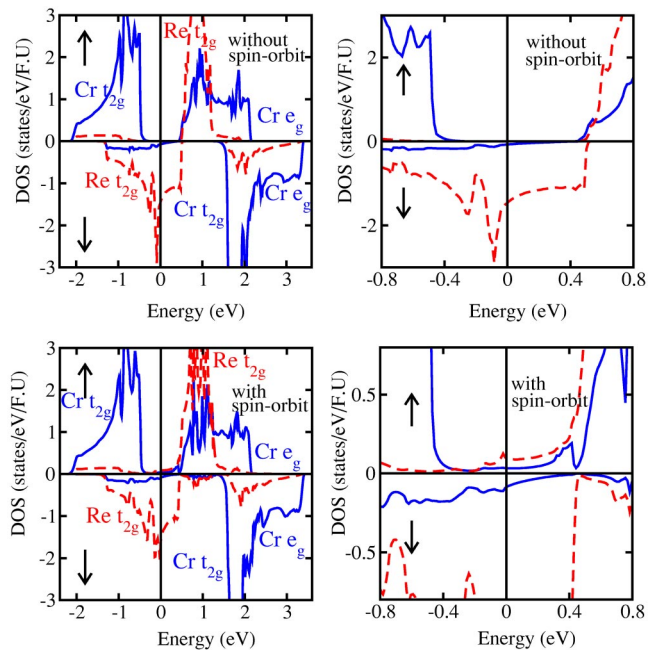


FIG. 1. (Color online) Orbital-resolved density of states (DOS) for  $\text{Sr}_2\text{CrReO}_6$ , without spin-orbit coupling (top row), and with spin-orbit coupling (bottom row). In the left-most panels the DOS is shown in an extended energy region and the symmetries of the peaks are indicated, whereas the right-most panels show a more detailed view of the DOS around the Fermi level.

see the bottom panel of Fig. 1. The carriers at the Fermi level remain highly polarized;  $D(\downarrow)/D(\uparrow) \sim 13$ , where  $D(\downarrow)$  and  $D(\uparrow)$  is the density of states at the Fermi level for minority and majority spin, respectively, instead of infinity as would be the case for a perfect half metal. As a first hint as to why the gap disappears, we note that in Re metal, the spin-orbit parameter  $\zeta(r)$  of the  $t_{2g}$  states in the spin-orbit Hamiltonian  $\hat{H}_{SO} = \zeta(r)\hat{\mathbf{l}} \cdot \hat{\mathbf{s}}$  is around 0.4 eV,<sup>10</sup> a number that decreases to approximately 0.3 eV in the double perovskite due to covalency.<sup>11</sup> Thus, the half-metallic gap and the spin-orbit parameter are of the same order, which makes it plausible that the spin-orbit splitting is capable of washing away the gap.

In order to understand in some more detail why the half-metallicity is destroyed, we analyze the density of states of this system, and work out why the spin-orbit coupling affects the DOS in this particular way. The basic critical ingredients in the DOS are the  $d$  states of the Cr and Re atoms, which in turn are split into  $t_{2g}$  and  $e_g$  states by the crystal field produced by the oxygen octahedra, with the  $t_{2g}$  states having lower energy and place for three electrons per spin channel, whereas the  $e_g$  states are higher in energy and have place for two electrons per spin channel. In the absence of spin-orbit coupling, the  $t_{2g}$  and  $e_g$  states are eigenstates to the Hamiltonian and do not hybridize with each other. Similarly, the spin channels do not hybridize with each other. (To be exact, the slight distortion of the oxygen octahedra introduces some very small extra splitting. We will however neglect this in the following.) In the scalar-relativistic DOS, the threefold degenerate Cr  $t_{2g}$  states of the majority spin channel are filled. Therefore, the Fermi level ends up in the crystal-field gap between the Cr  $t_{2g}$  and  $e_g$  states. A similar situation is seen in  $\text{Sr}_2\text{CrWO}_6$ .<sup>12,13</sup> Due to the antiferromagnetic coupling of Cr and Re, it is the minority spin channel in

Re which is the occupied one, and it contains two electrons. This means that the Re minority spin  $t_{2g}$  states are only filled to about two-thirds, resulting in a high DOS at the Fermi level in the minority spin channel. Due to hybridization, also the minority spin Cr  $t_{2g}$  states obtain a small occupation. In the majority spin channel, the Re  $d$  states are essentially empty; hybridization with the majority Cr  $t_{2g}$  states results nevertheless in a finite, small occupation. When spin-orbit coupling is included, the  $e_g$  and  $t_{2g}$  states are no longer eigenstates to the Hamiltonian, and they will therefore mix, as will the spin states. As a result, the high Re  $t_{2g}$  DOS at the Fermi level in the minority spin channel induces states in the majority spin channel. Since the spin-orbit parameter and the gap are both of the order of a few tenths of an electron volt, the result is that the half-metallic gap closes and the Cr  $t_{2g}$  and  $e_g$  peaks become connected. The induced pseudo-gap states have Re  $t_{2g}$  Cr  $e_g$ , as well as Cr  $t_{2g}$  character.

In summary, we have analyzed the electronic structure of the double perovskite  $\text{Sr}_2\text{CrReO}_6$ . The effect of spin-orbit coupling results in a rather large Re orbital moment and as a result, a total magnetic moment of  $1.28 \mu_B$ , whereas our predicted scalar-relativistic spin-only moment is precisely  $1.0 \mu_B$ . Furthermore, the large spin-orbit coupling in Re produces a nonvanishing DOS at the Fermi level in the majority spin channel, destroying the half-metallicity even at perfect ordering of the Cr and Re sites.

The authors acknowledge Professor O. K. Andersen for his valuable suggestions and critical reading of the manu-

script. G.V. and V.K. acknowledge the Max-Planck Society for the financial support. A.D. acknowledges financial support from Vetenskapsrådet (the Swedish Science Foundation) and the European Commission. Dr. H. Kato is acknowledged for sharing experimental details with us. P. Horsch and M. Alouani are acknowledged for their useful suggestions. J.M. Wills is acknowledged for letting us use his FP-LMTO code.

<sup>1</sup>J. Z. Sun, W. J. Gallagher, P. R. Duncombe, L. Krusin-Elbaum, R. A. Altman, A. Gupta, Yu Lu, G. O. Gong, and Gand Xiao, *Appl. Phys. Lett.* **69**, 3266 (1996).

<sup>2</sup>K. I. Kobayashi, T. Kimura, H. Sawada, K. Terakura, and Y. Tokura, *Nature (London)* **395**, 677 (1998).

<sup>3</sup>H. Kato, T. Okuda, Y. Okimoto, Y. Tomioka, Y. Takenoya, A. Ohkubo, M. Kawasaki, and Y. Tokura, *Appl. Phys. Lett.* **81**, 328 (2002).

<sup>4</sup>D. D. Sarma, P. Mahadevan, T. Saha-Dasgupta, S. Ray, and A. Kumar, *Phys. Rev. Lett.* **85**, 2549 (2000).

<sup>5</sup>H. Asano, N. Kozuka, A. Tsuzuki, and M. Matsui, *Appl. Phys. Lett.* **85**, 263 (2004).

<sup>6</sup>J. M. Wills, O. Eriksson, M. Alouani, and O. L. Price, in *Electronic Structure and Physical Properties of Solids*, edited by H. Dreyssé (Springer, Berlin, 2000).

<sup>7</sup>U. von Barth and L. Hedin, *J. Phys. C* **5**, 1629 (1972).

<sup>8</sup>J. P. Perdew, K. Burke, and M. Ernzerhof, *Phys. Rev. Lett.* **77**, 3865 (1996).

<sup>9</sup>H. Kato, T. Okuda, Y. Okimoto, Y. Tomioka, K. Oikawa, T. Kamiyama, and Y. Tokura, *Phys. Rev. B* **69**, 184412 (2004).

<sup>10</sup>L. F. Mattheiss, *Phys. Rev.* **151**, 450 (1966).

<sup>11</sup>O. K. Andersen (private communication).

<sup>12</sup>H. T. Jeng and G. Y. Guo, *Phys. Rev. B* **67**, 094438 (2003).

<sup>13</sup>J. B. Philipp, P. Majewski, L. Alff, A. Erb, R. Gross, T. Graf, M. S. Brandt, J. Simon, T. Walther, W. Mader, D. Topwal, and D. D. Sarma, *Phys. Rev. B* **68**, 144431 (2003).